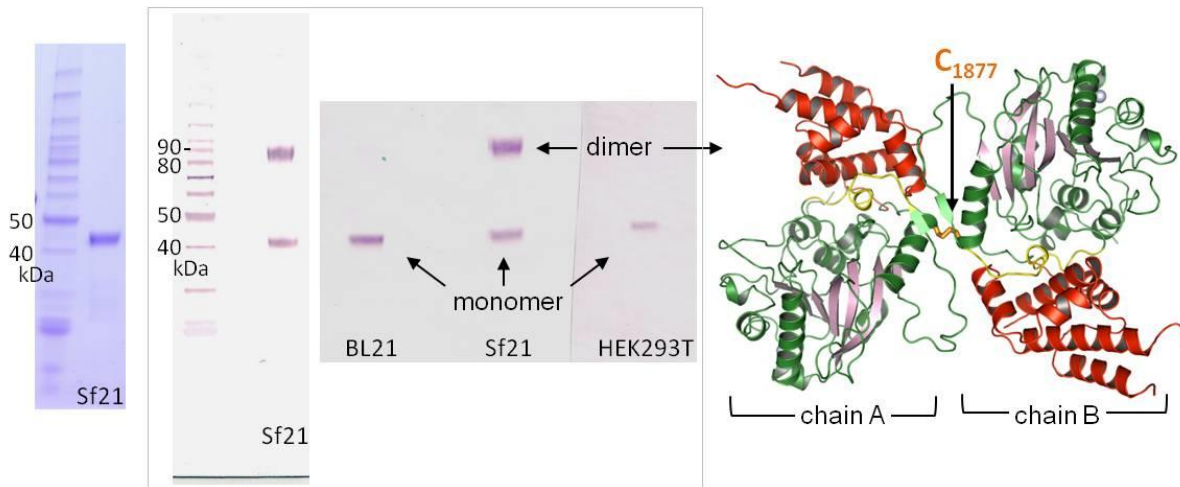


SUPPLEMENTARY INFORMATION

Supplementary Figure 1 : Recombinant CR-VI+ and dimer structure



Left: Coomassie-stained, reducing SDS-gel showing insect-cell derived CR-VI+ protein (2nd lane) running in between the 40 and 50 kDa protein marker (BenchMark, Invitrogen; 1st lane). The protein was purified using a single (chelating) chromatography step. Middle: Western blots of non-reducing SDS-gels. In insect cells (Sf21), CR-VI+ is produced as a mixture of monomers and dimers, whilst bacteria (BL21) and mammalian cells (HEK293T) only express monomers, suggesting that the dimeric form is an expression artefact. The blot at the left shows the non-reduced insect-cell derived protein next to the BenchMark protein ladder, with the dimeric form running between the 80 and 90 kDa marker. Yields from insect cells were much higher than those from bacteria and mammalian cells, and most experiments were therefore carried out with *Sf21*-derived CR-VI+. As the protein tended to aggregate at each purification step, no attempts were made to separate monomers from dimers, but reducing agent was added to reaction buffers used in activity studies. Right: Crystal structure of dimeric CR-VI+ obtained from *Sf21* cells, with the + domain in red, and the CR-VI domain in pink (β -strands) and green (helices and loops), except for $\lambda_{1650-1666}$ (yellow). The arrow indicates the inter-chain disulphide-bond linking the C₁₈₇₇ residues (orange).

Supplementary Figure 2 : Alignment of the C-termini of *L* proteins

PARAMYXOVIRIDAE

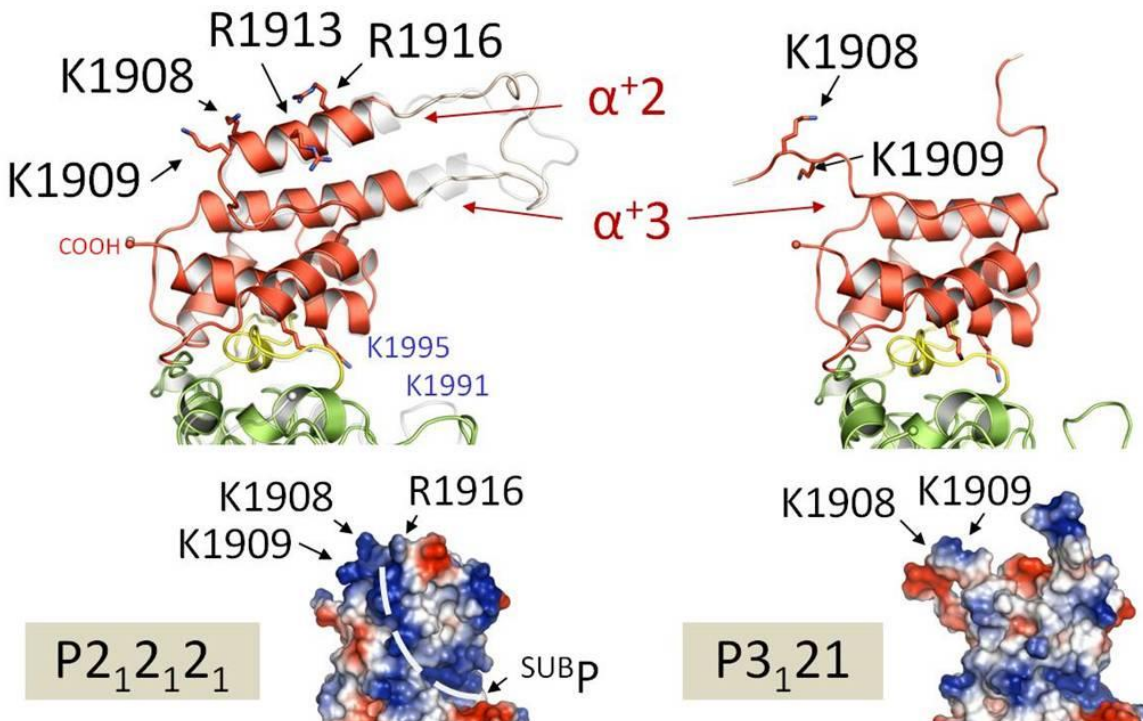
human Metapneumovirus	1894	-NLGNNAEIRKKLI KVTG YMLVS-	2003
avian Metapneumovirus	1984	-NLNSSELKKLV KVTG YILST-	2003
murine Pneumonia virus	2018	-SVSTSELKKV KVTG GILFRS-	2037
human Respiratory Syncytial virus	2142	-SLTTNEI KKL KITGSLLYN-	2161
bovine Respiratory Syncytial virus	2138	-SLTTNEI KKL K V TGSVLYS-	2157
Sendai virus	2184	-RFLTKEIKILM KILG AVKMF-	2203
Tupaia virus	2250	-AIITKEIKLW WKKL IGYSYLL-	2269
Measles virus	2262	-KVTVKET EWEY KLVGYSALI-	2281
Rinderpest virus	2162	-KLTTKE EWEF KLIGYSALI-	2181
Canine Distemper virus	2162	-QLETKE EWEF KLIGYSALI-	2181
Narivavirus	2182	-HMTPRE EIKLWW KAISYSFLV-	2201
Mossman virus	2182	-PITTPEAK MWWK AIGYSVLM-	2201
Nipah virus	2225	-DLSNREV KIWW KIIGYISII-	2244
J virus	2182	-NLSTPEV KIWW KIVGYSVLY-	2201
Beilong virus	2150	-PLPTAEV KIWW KIVGYSVLH-	2169
Tailam virus	2150	-PLQTAEV KVWW KIVGYSVLH-	2169
Newcastle Disease virus	2178	-YLTRAQQ KFYMK TICNAAKG-	2197
Tuhoko virus 1	2224	-YLSRAQQ KRVWKSVC SVILT-	2243
Tuhoko virus 2	2218	-EFQRSE QKKLWKN ICCIAFI-	2237
Tuhoko virus 3	2220	-LLSRAE QKTWQK IQIGAINLV-	2239
Mapuera virus	2206	-QFSRSQQ KQIWK AIGCSALV-	2225
human Parainfluenza virus 3	2188	-WFLTKEV RILMK LGAKLL-	2207
human Parainfluenza virus 4b	2222	-KLSRPK QKQIWK ILCCTLFV-	2241
porcine Rubulavirus	2206	-FLSRPM QKRVWKT TICCALME-	2225
simian virus 41	2218	-PIHRSY QKRIWKA LCVIYC-	2237
Mumps virus	2212	-LLNRAY QKRIWKA ICCVIYC-	2231
Menangle virus	2220	-FLDRPT QKRIWKS VGSVILE-	2239
Tioman virus	2222	-KLDRSE QKRIWKA IGSVILS-	2241
Fer-de-lance virus	2159	-EITNRD DKKKLF KLICSAFYF-	2178
avian Paramyxovirus 4	2185	-NKARDFF KRRLK LVGFSLCG-	2204
avian Paramyxovirus 5	2241	-TLTRHEV KLF IKYLGSIKG-	2260
avian Paramyxovirus 7	2206	-MLSRSET KLLIK VLSSAAWKG-	2225
avian Paramyxovirus 8	2218	-VLTRAEV KVCIK FLGAIIKL-	2237

FILOVIRIDAE

Sudan Ebolavirus	2182	-RMSDAE I KLMD R LTSLVNMF-	2201
Zaire Ebolavirus	2185	-RMQDSE V RLIER R LT G LLSLF-	2204
Tai Forest Ebolavirus	2185	-RMQDSE I KL I D R LT G LLSLC-	2204
Reston Ebolavirus	2183	-RLRDAE I KLIER R LT G LMRFY-	2202
Marburg virus	2300	-NTKIAE Q LLN R VIC Y ILFF-	2319
Lloviu Cuevavirus	2173	-RTDQAER R LLN R L V GLVQFF-	2192

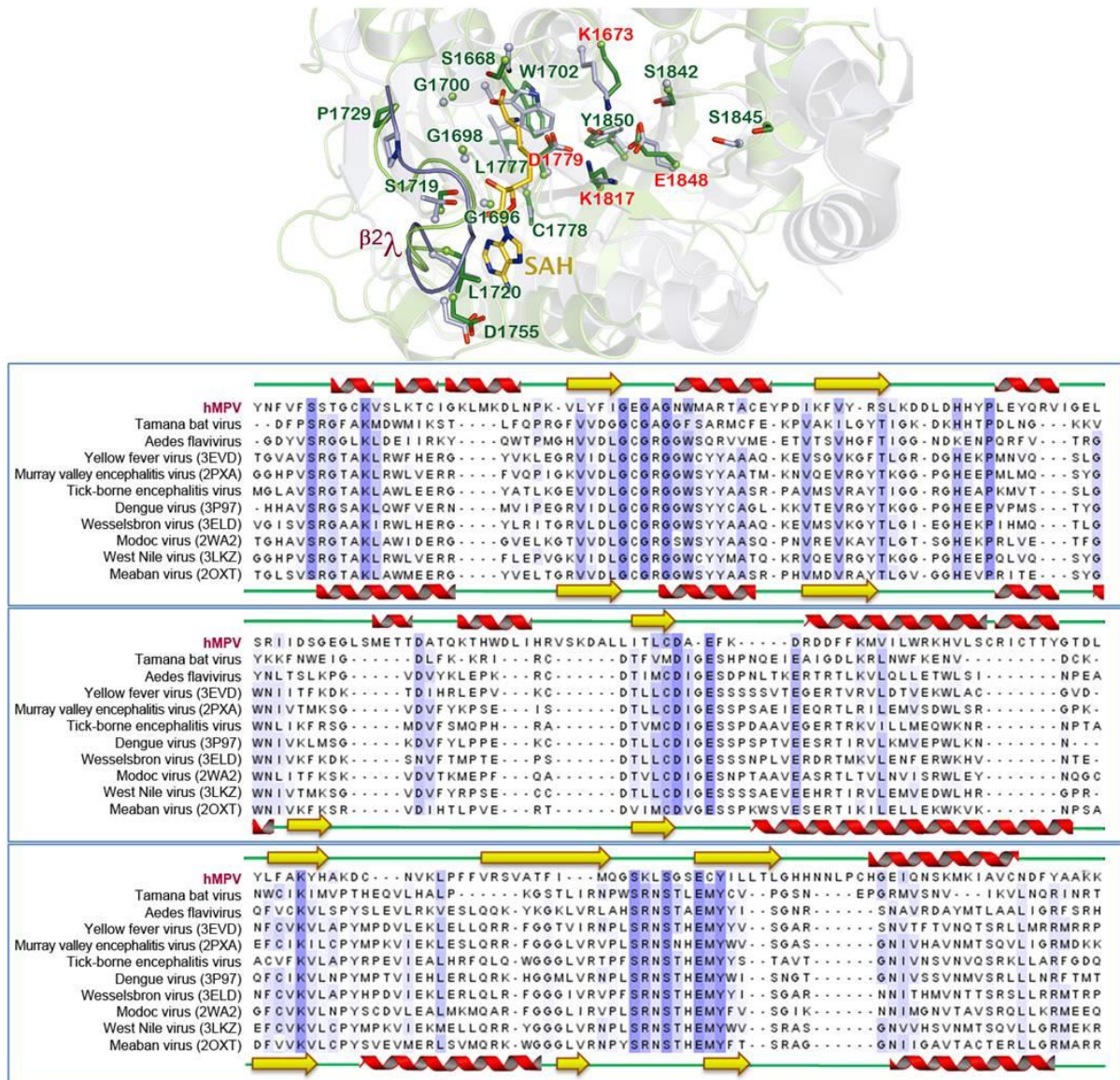
Alignment of members of the *Paramyxo-* and *Filoviridae*, showing the conserved K-K-G motif (the second lysine in the motif is replaced by an arginine in *Filoviridae*). Members of the *Pneumovirinae* subfamily are listed in blue. The motif is not obvious in *Rhabdoviridae*, *Nyaviridae* or *Bornaviridae* *L* proteins.

Supplementary Figure 3 : Plasticity of the + domain at the height of the $\alpha^{+}2$ - $\alpha^{+}3$ transition



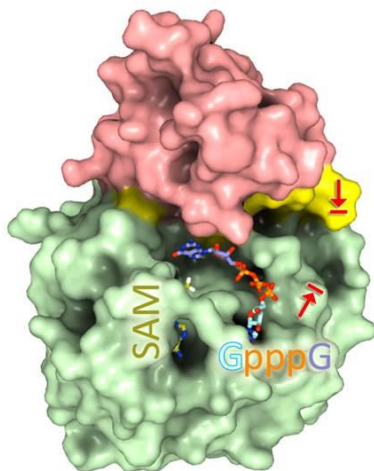
The cartoons show the varying lengths of the helices in $P_{2_1}2_12_1$ structures (left; red helices correspond to PDB 4UCI, white helices to 4UCY) and the complete absence of α^+2 in a $P_{3_1}2_1$ structure (right; 4UD0). The basic residues of α^+2 are shown as sticks, as are K_{1991} and K_{1995} of the K-K-G motif. The loops linking the helices in the $P_{2_1}2_12_1$ structures are representative since the electron-density is somewhat diffuse. The cartoons further illustrate the close connection of $\lambda_{1650-1666}$ (in yellow) to the + domain, and its disengagement from CR-VI (green). The dramatic effect of the plasticity on the surface characteristics of the + domain is shown underneath the cartoons. The surfaces are coloured according to their basic (blue) or acidic (red) charges. The dashed white line follows a basic region extending from the RNA-binding site (^{SUB}P) up to the α^+2 helix in PDB 4UCI, which dissolves as the helix unwinds.

Supplementary Figure 4 : Structural alignment to flavivirus MTases



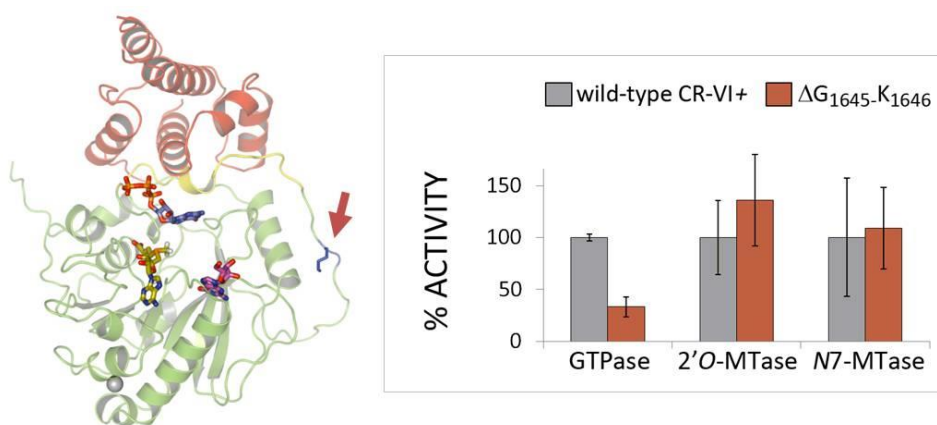
Structural overlay of CR-VI+ (green) onto the Yellow Fever virus MTase (PDB 3EVF; light blue), with identical residues (which predominantly cluster around ^{SAM}P) shown as sticks. Centrally to the K-D-K-E tetrad (red residue labels) lays tyrosine (Y₁₈₅₀), a conserved residue of Rrmj-type MTases. The long $\beta^2\lambda$ loop is highlighted. The alignment corresponding to the overlay is shown underneath, and includes additional flavivirus MTases. PDB codes are given between brackets, where available. The alignment covers residues 1663-2005 of hMPV L and 51-247 of the flavivirus sequences (PDB-files numbering). The secondary structure elements of CR-VI+ are given on top of the alignment, those of flavivirus MTases at the bottom (loops are in green, β -strands in yellow and α -helices in red).

Supplementary Figure 5 : The role of ^{NS}P



Surface presentation of CR-VI+ (colour scheme as in Figure 6a). Although co-crystals of CR-VI+ with cap analogues could not be obtained, GpppG can be modelled into the protein with G (light blue) occupying ^{NS}P and the N1 nucleotide (purple) occupying ^{SUB}P. In other MTases, a narrow, high-affinity cap-binding site is found in the space between the arrows.

Supplementary Figure 6 : Involvement of the long, N-terminal loop in GTPase activity



Removing N-terminal-loop residues G₁₆₄₅ and K₁₆₄₆ (indicated by the arrow in the structure) resulted in a marked reduction in GTPase activity, without affecting the MTase reactions, suggesting the mutation did not alter the overall structure (the activities of wild-type CR-VI+ were set at 100%; measurements were carried out as in Figs. 3b and 4; the bars and error bars correspond to the mean values from 3 measurements and their standard deviations, respectively). The N-terminal loop may be directly involved in the GTPase reaction (e.g. by folding over a nearby site containing the substrate), or indirectly (e.g. by restricting the flexibility of λ₁₆₅₀₋₁₆₆₆ and thus the movement of the + domain relative to the MTase domain).

Supplementary Figure 7 : Synthetic gene and primers used for mutagenesis

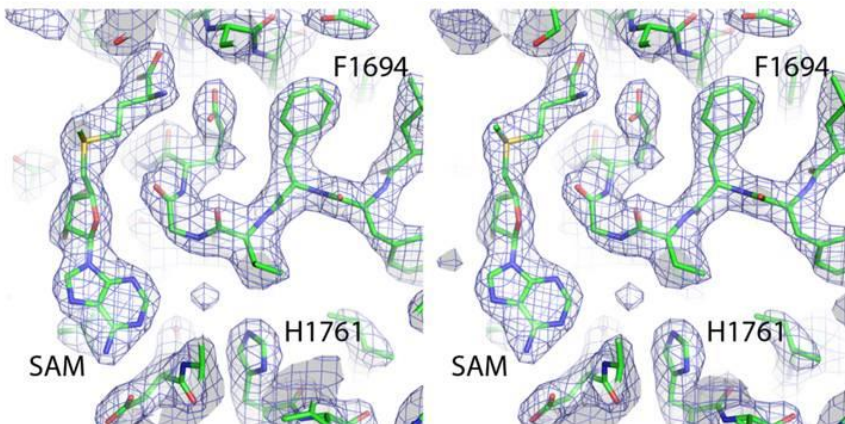
atggctctgctgaccctatccctccatggtaacctgacccaagtgtcgacccc
M A L L T P I P S P M V N L T Q V I D P 1618
accgagcagctggctacttcccaagatcaccccgacgcctgaagaactacgacact
T E Q L A Y F P K I T F E R L K N Y D T 1638
tcctccaactacgtaaggcaagctgaccgtactacatgatccgtgcgcggcggcag
S S N Y A K G K L T R N Y M I L L P W Q 1658
cacgtgaaccgttacaacttgcgttccaggcaccgggtcaagggtcactcaagacc
H V N R Y N F V F S S T G C K V S L K T 1678
tgcatcgcaagctgtatgaaaggactgaaccccaagggtgtacttcatcgccgggt
C I G K L M K D L N P K V L Y F I G E G 1698
gctggcaactggatggctgtaccgcttgcgagttacccgacatcaagttgtgtaccgt
A G N W M A R T A C E Y P D I K F V Y R 1718
tccctgaaggacgacccactcgaccactacccctcgagttaccaggcgtgtatcgccgag
S L K D D L D H Y P L E Y Q R V I G E 1738
ctgtcccgatcatcgactccggcgaggccgtctatggaaaccaccgacgtacccaa
L S R I I D S G E G L S M E T T D A T Q 1758
aagaccactgggacactgtatccaccgtgttccaaaggacgcggccgtgtatccgtgc
K T H W D L I H R V S K D A L L I T L C 1778
gacgtgaggtaaggacgtgacacttcaagatggcatccgtggcgaagcac
D A E F K D R D F F K M V I L W R K H 1798
gtgtgtctccgtatctgcaccacttgcggcaccgttccgtgttccgttaactgac
V L S C R I C T T Y G T D L Y L F A K Y 1818
cacgctaaggactgcaacgtgaaagctgcgttccgtgttccgttccatc
H A K D C N V K L P F F V R S V A T F I 1838
atgcaagggttccaagctgtccgggttccgagtgttccatc
M Q G S K L S G S E C Y I L L T L G H H 1858
aacaacctgcctgcacggcagatccagaacacgcaagatgcgcgtgtcaac
N N L P C H G E I N S K M K I A V C N 1878
gacttctacgtcataagaagctggacaacaagacatcgaggactactgcaaggcc
D F Y A A K K L D N K S I E A N C K S L 1898
ctgtccggcctgcgtatccccatcaacaagaactcaaccgtcagcgtgcctgt
L S G L R I P I N K K E L N R Q R R L L 1918
accctccagtccaaaccactccctgtggctaccgtggcgttctaaggatcgact
T L Q S N H S S V A T V G G S K V I E S 1938
aagtggctaccacaaggccaaaccatcatcgactggctcgagcacatccgt
K W L T N K A N T I I D W L E H I L N S 1958
cccaaggcgcagactgaaactacgacttctcgaggcttcgagaacacccat
P K G E L N Y D F F E A L E N T Y P N M 1978
atcaagctcatcgacaacctggcaacgctgaaatcaagaagttgtatcaagg
I K L I D N L G N A E I K K L I K V T G 1998
tacatgtgttccaaagaagtcggacaccatcaccatcatcactgtat
Y M L V S K K **S G H H H H H H** 2013

mutant	forward primer (from 5' to 3')	reverse primer (from 5' to 3')
Q1658A	TATAATGCAGTGGCTCACGTGAACCGTTACAACCTTC	TATAATGCAGTGGCCAGGGCAAGCAGGATC
H1659A	ATAT GCTCTTC AGCTGTGAACCGTTACAACCTTCGTG	ATAT GCTCTTC AAGCCTGCCAGGGCAGCAG
R1662A	ATAT GCTCTTC AGCTTACAACCTCGTGTCTCCAGCAC	ATAT GCTCTTC AAGCGTTCACGTGCTGCCAGG
R1662E	ATAT GCTCTTC AGAGTACAACCTCGTGTCTCCAGCAC	ATAT GCTCTTC ACTCGTTCACGTGCTGCCAGG
R1662Q	ATAT GCTCTTC ACAGTACAACCTCGTGTCTCCAGCAC	ATAT GCTCTTC ACTGGTTCACGTGCTGCCAG
F1665A	TATAATGCAGTGGCTTCCAGCACCGGTTGC	TATAATGCAGTGGCACGAAGTTGTAACGGTTCAC
S1668A	TATAATGCAGTGGCTAGCACCGGTTGCAAGG	TATAATGCAGTGGCGAACACGAAGTTGTAACGGTTC
S1669A	TATAATGCAGTGGCTACCGGTTGCAAGGTGTC	TATAATGCAGTGGGGAGAACACGAAGTTGTAACG
T1670A	ATAT GCTCTTC AGCTGGTTGCAAGGTGCACTCAAG	ATAT GCTCTTC AAGCGCTGGAGAACACGAAGTTGTAAC
K1673A	TATAATGCAGTGGCTGTGCACTCAAGACCTGCATC	TATAATGCAGTGGCGAACACGGGTGCTGG
E1697C	TATAATGCAGTGGCGTGCGCAACTGGATG	TATAATGCAGTGGCGAGCCGATGAAGTACAGC
H1727A	TATAATGCAGTGGCTACCCCTCGAGTACAG	TATAATGCAGTGGCGTGTGAGGTGCTCC
D1779A	ATAT GCTCTTC AGCTGCTGAGTTCAAGGACCGTG	ATAT GCTCTTC AAGCGCACAGGGTATCAGC
D1779Q	ATAT GCTCTTC ACAGGCTGAGTTCAAGGACCGTG	ATAT GCTCTTC ACTGGCACAGGGTATCAGCAG
E1781A	TATAATGCAGTGGCTGTTCAAGGACCGTGACGAC	TATAATGCAGTGGCGTGCACAGGGT
E1781Q	TATAATGCAGTGGCTAGTTCAAGGACCGTGACGAC	TATAATGCAGTGGCGACAGGGT
R1785A	TATAATGCAGTGGCTGACGACTTCTCAAGATGGTATC	TATAATGCAGTGGCGTCTTGAACCTCAGCGTC
K1817A	TATAATGCAGTGGCTTACACGCTAAGGACTGCAAC	TATAATGCAGTGGCGAACAGGTACAGGTG
K1817Q	TATAATGCAGTGGCTAACACACGCTAAGGACTGCAAC	TATAATGCAGTGGCGAACAGGTACAGGTG
K1821Q	ATAT GCTCTTC ACAGGACTGCAACGTGAAGCTG	ATAT GCTCTTC ACTGACGGTGGTACTTAGCGAACAGG
S1842A	ATAT GCTCTTC AGCTAAGCTGGCTCCGGTTCCGAG	ATAT GCTCTTC AAGCACCTTGATGAGGTAGCC
K1843A	ATAT GCTCTTC AGCTGTGCGGTCCGGAGTGTAC	ATAT GCTCTTC AAGCGAACCTTGATGATGAAGG
E1848A	ATAT GCTCTTC AGCTTGCTACATCTGCTCACCC	ATAT GCTCTTC AAGCGAACCCGACAGCTTG
C1877A	TATAATGCAGTGGCTAACGACTTCTACGCTGCTAAAGAAG	TATAATGCAGTGGCACGGCGATCTTCATCTTG
K1991E	ATAT GCTCTTC AGAGAAGTTGATCAAGGTACCG	ATAT GCTCTTC ACTCGATTTCAGCGTTGCC

K1991Q	ATAT GCTCTTC ACAGAAGTTGATCAAGGTACCG	ATAT GCTCTTC ACTGGATTTCAGCGTTGCC
K1992Q	ATAT GCTCTTC ACAGTGTGATCAAGGTACCGG	ATAT GCTCTTC ACTGCTTGATTTCAGCGTTGCC
K1995Q	ATAT GCTCTTC CACAGGTACCCGCTACATG	ATAT GCTCTTC ACTGGATCAACTCTTGATTTCAGCG
K1995E	ATAT GCTCTTC AGAGGTACCCGCTACATG	ATAT GCTCTTC ACTCGATCAACTCTTGATTTCAGCG
K1991Q/K1992Q	TATAATGCAGTGGCAGTTGATCAAGGTACCGG	TATAATGCAGTGGCTGGATTTCAGCGTTGCC
K1991Q/K1995Q	TATAATGCAGTGTGATCCAGAAGTTGATCCAGG	TATAATGCAGTGTGATTCAGCGTTGCCAG
K1991Q/K1992Q/K1995Q	TATAATGCAGTGGCAGTTGATCCAGGTACCCG	TATAATGCAGTGGCTGGATTTCAGCGTTGCC
ΔG1645K1646	TATAATGCAGTGGCTAACGCTGACCCGTAACATGATC	TATAATGCAGTGGCTAGTTGGAGGAAGTGTG

The nucleotide sequence of the synthetic gene for the CR-VI+ domain is shown on top, with the corresponding protein sequence underneath. Residues that are not in the original hMPV *L* protein (the start methionine, the adjacent alanine, and the oligo-histidine-tag) are in bold and italic. The table lists the primers used to generate mutants. The *BtsI* and *BspQI* recognition sequences are highlighted in gray and yellow, respectively.

Supplementary Figure 8 : Electron density map



The stereo image shows the electron density of the SAM-binding site of the CR-VI+ structure (PDB: 4UCI, chain A). The 2Fo-Fc map was contoured at 1.5 sigma.